A Geometrical Notation for Stacking Faults in Close-Packed Structures

By Dhananjai Pandey

School of Materials Science and Technology, Banaras Hindu University, Varanasi-221005, *India*

Abstract

A new geometrical notation based on the use of intrinsic–extrinsic classification in conjunction with the concept of assigning subscripts to close-packed layers with different environments is proposed. The terms intrinsic and extrinsic have been used in a purely geometrical sense and are not linked with specific formation processes for stacking faults. It is shown that the proposed notation can provide a very compact and unique way of representing fault configurations in all close-packed structures, including the long-period polytypes.

Several different notations* have been used for representing stacking faults in close-packed structures, none of which can provide a compact and unambiguous notation (see Pandey & Krishna, 1981, 1982). An alternative notation, which is based on the use of intrinsic–extrinsic classification (Frank, 1951) in conjunction with the concept of assigning subscripts to different close-packed layers (Prasad & Lele, 1971; Pandey & Krishna, 1976), is proposed. In this notation, the terms intrinsic and extrinsic have been used in a purely geometrical sense in accordance with the original suggestion of Frank and not by associating these terms with specific processes of formation like condensation of a sheet of vacancies and interstitials respectively. As shown below, this notation can provide a very compact and unique way of representing fault configurations in all close-packed structures including long-period structures observed in polytypic materials. We shall develop this notation in relation to the possible fault configurations in a hexagonal structure, namely 6H ABCACB, which is the most common high-temperature modification of SiC. An application of this notation to a rhombohedral structure, namely 9R, is also presented.

---

* For a detailed account of the various notations, the reader is referred to the paper *Stacking Faults in Close-Packed Structures: Definitions and Notations* (Contents: Introduction; Existing Notations: Growth and Deformation Faults, Extrinsic and Intrinsic Faults, The 'Δ–∇' Notation, The 'h–k' Notation; Present Notation; Application of the Notation; Conclusion) by D. Pandey. This paper has been deposited with the British Library Lending Division as Supplementary Publication No. SUP 39176 (23 pp.). Copies may be obtained through The Executive Secretary, International Union of Crystallography, 5 Abbey Square, Chester CH1 2HU, England.
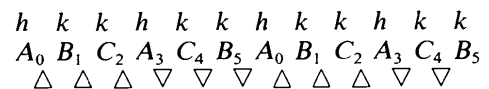
Table 1. *Possible fault configurations in the* 6H *($A_0B_1C_2A_3C_4B_5,\ldots$) structure*

Fault configuration ABC sequence	Subscript notation
... A B C A C B A_0 ⋮ C_0 A B C B A C ...	$I_{0,0}$
... A B C A C B A_0 ⋮ C_1 A B A C B C ...	$I_{0,1}$
... A B C A C B A_0 ⋮ C_2 A C B A B C ...	$I_{0,2}$
... A B C A C B A_0 ⋮ C_3 B A C A B C ...	$I_{0,3}$
... A B C A C B A_0 ⋮ C_4 B A B C A C ...	$I_{0,4}$
... A B C A C B A_0 ⋮ C_5 B C A B A C ...	$I_{0,5}$
... A B C A C B A B_1 ⋮ A_0 B C A C B A ...	$I_{1,0}$
... A B C A C B A B_1 ⋮ A_1 B C B A C A ...	$I_{1,1}$
... A B C A C B A B_1 ⋮ A_2 B A C B C A ...	$I_{1,2}$
... A B C A C B A B_1 ⋮ A_3 C B A B C A ...	$I_{1,3}$
... A B C A C B A B_1 ⋮ A_4 C B C A B A ...	$I_{1,4}$
... A B C A C B A B_1 ⋮ A_5 C A B C B A ...	$I_{1,5}$
... A B C A C B A B C_2 ⋮ B_0 C A B A C B ...	$I_{2,0}$
... A B C A C B A B C_2 ⋮ B_1 C A C B A B ...	$I_{2,1}$
... A B C A C B A B C_2 ⋮ B_2 C B A C A B ...	$I_{2,2}$
... A B C A C B A B C_2 ⋮ B_3 A C B C A B ...	$I_{2,3}$
... A B C A C B A B C_2 ⋮ B_4 A C A B C B ...	$I_{2,4}$
... A B C A C B A B C_2 ⋮ B_5 A B C A C B ...	$I_{2,5}$
... A B C A C B A A_0 ⋮ C B C A C B A ...	E_0
... A B C A C B A B_1 ⋮ A C A C B A ...	E_1
... A B C A C B A B C_2 ⋮ B A C B A B C ...	E_2

Note: dotted vertical lines represent the location of the fault plane with respect to the initial stacking sequence on the left-hand side.

Enantiomorphous pairs: $I_{0,1}$ & $I_{2,3}$, $I_{0,2}$ & $I_{1,3}$, $I_{1,1}$ & $I_{2,2}$, $I_{1,4}$ & $I_{2,5}$, and E_0 & E_2.

The 6H ($ABCACB,\ldots$) structure can also be written as $hkkhkk,\ldots$ or as $\triangle\triangle\triangle\triangledown\triangledown\triangledown,\ldots$ in the 'h–k' and 'Δ–∇' notations (for details see Pandey & Krishna, 1982). Six kinds of layers need to be distinguished in the perfect 6H structure of which three layers are in the $\triangle$ orientation with respect to the preceding layers and the remaining three in the $\triangledown$ orientation. Let us choose the origin on an 'h' type layer which is followed by two 'k' layers such that the layer next to the origin is in the $\triangle$ orientation. Let the layer through the origin be denoted by a subscript 0 and succeeding layers in the unit cell by subscripts 1, 2, 3, 4 and 5. Then the perfect 6H structure can be written as

$$
\begin{array}{cccccccccccc}
h & k & k & h & k & k & h & k & k & h & k & k \\
A_0 & B_1 & C_2 & A_3 & C_4 & B_5 & A_0 & B_1 & C_2 & A_3 & C_4 & B_5 \\
\triangle & \triangle & \triangle & \triangledown & \triangledown & \triangledown & \triangle & \triangle & \triangle & \triangledown & \triangledown &
\end{array}
$$

There are six ways in which layers in the unit cell of the 6H structure can be written with the first layer in A orientation: (i) $A_0B_1C_2A_3C_4B_5$, (ii) $A_1B_2C_3B_4A_5C_0$, (iii) $A_2B_3A_4C_5B_0C_1$, (iv) $A_3C_4B_5A_0B_1C_2$, (v) $A_4C_5B_0C_1A_2B_3$, (vi) $A_5C_0A_1B_2C_3B_4$. Similarly there are six ways in which the structure of 6H can be written starting with the

Table 2. *Intrinsic fault configurations in the* $9R$ $(A_0B_1A_2C_0A_1C_2B_0C_1B_2,\ldots)$ *structure*

Fault configuration ABC sequence		Subscript notation
… $A\ B\ A\ C\ A\ C\ B\ C\ B\ A_0$ ⋮ $C_0\ A$	$C\ B\ C\ B\ A\ B\ A$ …	$I_{0,0}$
… $A\ B\ A\ C\ A\ C\ B\ C\ B\ A_0$ ⋮ $C_1\ B$	$A\ B\ A\ C\ A\ C\ B$ …	$I_{0,1}$
… $A\ B\ A\ C\ A\ C\ B\ C\ B\ A_0$ ⋮ $C_2\ B$	$C\ B\ A\ B\ A\ C\ A$ …	$I_{0,2}$
… $A\ B\ A\ C\ A\ C\ B\ C\ B\ A_0$ ⋮ $C_{\bar0}\ B$	$C\ A\ C\ A\ B\ A\ B$ …	$I_{0,\bar0}$
… $A\ B\ A\ C\ A\ C\ B\ C\ B\ A_0$ ⋮ $C_{\bar1}\ A$	$B\ A\ B\ C\ B\ C\ A$ …	$I_{0,\bar1}$
… $A\ B\ A\ C\ A\ C\ B\ C\ B\ A_0$ ⋮ $C_{\bar2}\ A$	$C\ A\ B\ A\ B\ C\ B$ …	$I_{0,\bar2}$
… $A\ B\ A\ C\ A\ C\ B\ C\ B\ A\ B_1$ ⋮ C_0	$A\ C\ B\ C\ B\ A\ B\ A$ …	$I_{1,0}$
… $A\ B\ A\ C\ A\ C\ B\ C\ B\ A\ B_1$ ⋮ C_1	$B\ A\ B\ A\ C\ A\ C\ B$ …	$I_{1,1}$
… $A\ B\ A\ C\ A\ C\ B\ C\ B\ A\ B_1$ ⋮ C_2	$B\ C\ B\ A\ B\ A\ C\ A$ …	$I_{1,2}$
… $A\ B\ A\ C\ A\ C\ B\ C\ B\ A\ B_1$ ⋮ $C_{\bar0}$	$B\ C\ A\ C\ A\ B\ A\ B$ …	$I_{1,\bar0}$
… $A\ B\ A\ C\ A\ C\ B\ C\ B\ A\ B_1$ ⋮ $C_{\bar1}$	$A\ B\ A\ B\ C\ B\ C\ A$ …	$I_{1,\bar1}$
… $A\ B\ A\ C\ A\ C\ B\ C\ B\ A\ B_1$ ⋮ $C_{\bar2}$	$A\ C\ A\ B\ A\ B\ C\ B$ …	$I_{1,\bar2}$
… $A\ B\ A\ C\ A\ C\ B\ C\ B\ A\ B\ A_2$ ⋮ B_0	$C\ B\ A\ B\ A\ C\ A\ C$ …	$I_{2,0}$
… $A\ B\ A\ C\ A\ C\ B\ C\ B\ A\ B\ A_2$ ⋮ B_1	$A\ C\ A\ C\ B\ C\ B\ A$ …	$I_{2,1}$
… $A\ B\ A\ C\ A\ C\ B\ C\ B\ A\ B\ A_2$ ⋮ B_2	$A\ B\ A\ C\ A\ C\ B\ C$ …	$I_{2,2}$
… $A\ B\ A\ C\ A\ C\ B\ C\ B\ A\ B\ A_2$ ⋮ $B_{\bar0}$	$A\ B\ C\ B\ C\ A\ C\ A$ …	$I_{2,\bar0}$
… $A\ B\ A\ C\ A\ C\ B\ C\ B\ A\ B\ A_2$ ⋮ $B_{\bar1}$	$C\ A\ C\ A\ B\ A\ B\ C$ …	$I_{2,\bar1}$
… $A\ B\ A\ C\ A\ C\ B\ C\ B\ A\ B\ A_2$ ⋮ $B_{\bar2}$	$C\ B\ C\ A\ C\ A\ B\ A$ …	$I_{2,\bar2}$

Enantiomorphous pairs: $I_{0,\bar0}$ & $I_{1,\bar1}$, $I_{0,\bar1}$ & $I_{1,\bar2}$, $I_{0,\bar2}$ & $I_{2,\bar1}$, and $I_{1,2}$ & $I_{2,0}$.

first layer in the B position and six starting with C. It is possible for the intrinsic fault to commence at any one of the six layer positions in the $6H$ unit cell. Corresponding to each of these possibilities there are six different ways which the subsequent $6H$ sequence may follow. This provides a total of 36 possibilities. Half of these are identical with the other half since they are related by a rotation of 60° around [00.1]. The remaining 18 fault configurations occurring after layers with subscripts 0, 1 and 2 are listed in Table 1. The dotted vertical line indicates the location of the fault plane with respect to the initial stacking sequence on the left-hand side. It is evident from the table that the subscripts of two layers, one on each side of the fault plane, can uniquely specify the fault configuration. So we can represent each intrinsic fault configuration listed in Table 1 by symbols like $I_{r,s}$ where r and s correspond to the subscript of the layers on the left- and right-hand side of the fault plane and I stands for intrinsic. The identical nature of fault configurations occurring after layers with subscripts 0,1,2 and 3,4,5 can now be expressed mathematically as: $I_{r,s} = I_{(r+3)\mod 6,(s+3)\mod 6}$. Of the 18 intrinsic fault configurations listed in Table 1, $I_{0,1}$, $I_{0,2}$, $I_{1,1}$ and $I_{1,4}$ are enantiomorphous with $I_{2,3}$, $I_{1,3}$, $I_{2,2}$ and $I_{2,5}$ respectively, leaving only 14 unique intrinsic fault configurations in the $6H$ structure.

If one considers the insertion of one additional layer of atoms in the $6H$ structure, one obtains six extrinsic fault configurations, half of which are identical to the other half since they are related by a rotation through 60° about [00.1]. The remaining three fault configurations are also listed in Table 1 and are represented by symbols like E_r where r stands for the subscript of the layer after which an additional layer has been inserted. Since E_2 is enantiomorphous with E_0, there are only two unique extrinsic fault configurations E_0 and E_1 in the $6H$ structure obtained by inserting a single additional layer after various layer positions of the $6H$ unit cell.

The application of the present notation to the possible intrinsic fault configurations in a rhombohedral $9R$ structure is illustrated below. The $9R$ or hhk structure can be written in two ways.

(i)

$$
\begin{array}{ccccccccc}
h & h & k & h & h & k & h & h & k \\
\ldots\ A_0 & B_1 & A_2 & C_0 & A_1 & C_2 & B_0 & C_1 & B_2\ \ldots \\
\triangle & \triangledown & \triangledown & \triangle & \triangledown & \triangledown & \triangle & \triangledown &
\end{array}
$$

(ii)

$$
\begin{array}{ccccccccc}
h & h & k & h & h & k & h & h & k \\
\ldots\ A_{\bar0} & C_{\bar1} & A_{\bar2} & B_{\bar0} & A_{\bar1} & B_{\bar2} & C_{\bar0} & B_{\bar1} & C_{\bar2}\ \ldots \\
\triangledown & \triangle & \triangle & \triangledown & \triangle & \triangle & \triangledown & \triangle &
\end{array}
$$

These structures are indistinguishable since they are related to each other by a rotation of 60° about [00.1]. The two structures can be distinguished only when both occur in the same crystal. For the $\triangle\triangledown\triangledown$ sequence, we choose our origin on an 'h' layer which is followed by another 'h' layer such that the latter is in $\triangle$ orientation with respect to the origin layer. We assign subscripts 0 to the origin layer and subscripts 1 and 2 to the two succeeding layers. For the $\triangledown\triangle\triangle$ sequence, the origin is chosen on an 'h' layer which is followed by another 'h' such that the latter is in $\triangledown$ orientation with respect to the origin layer. Let the origin layer be denoted by subscript $\bar0$ and the succeeding two layers by $\bar1$ and $\bar2$. Stacking faults can occur after any of the six kinds of layers but the fault configurations occurring after the 0, 1 and 2 type layers are identical to those occurring after the $\bar0$, $\bar1$ and $\bar2$ type layers. An intrinsic fault would mark the beginning of a fresh $9R$ sequence which can be written in six different ways with the first layer in A, B or C positions, three corresponding to the sequence $\triangle\triangledown\triangledown$ and three to the sequence $\triangledown\triangle\triangle$, leading to a total of 18 possible intrinsic fault configurations in the $9R$ ($\triangle\triangledown\triangledown$) structure which are listed in Table 2 along with their subscript notation. It can be shown that

the fault configurations $I_{0,\bar{0}}$, $I_{0,\bar{1}}$, $I_{0,\bar{2}}$ and $I_{1,2}$ are enantiomorphous with $I_{1,\bar{1}}$, $I_{1,\bar{2}}$, $I_{2,\bar{1}}$ and $I_{2,0}$ respectively, leaving only 14 unique intrinsic fault configurations in the $9R$ structure.

References

FRANK, F. C. (1951). *Philos. Mag.* **42**, 809–819.
PANDEY, D. & KRISHNA, P. (1976). *Acta Cryst.* A32, 488–492.
PANDEY, D. & KRISHNA, P. (1981). *Ind. J. Pure Appl. Phys.* **19**, 796–802.
PANDEY, D. & KRISHNA, P. (1982). In *Current Topics in Materials Science*, Vol. 9, edited by E. KALDIS. Amsterdam: North-Holland.
PRASAD, B. & LELE, S. (1971). *Acta Cryst.* A27, 54–64.

Cell Volumes of APO_4, AVO_4, and $ANbO_4$ Compounds, where A = Sc, Y, La–Lu*

By A. T. ALDRED

Materials Science and Technology Division, Argonne National Laboratory, Argonne, IL 60439, USA

Abstract

Precision lattice constants have been determined for a series of APO_4, AVO_4, and $ANbO_4$ compounds (where A is a rare-earth ion, Sc, Y, or La) with the monazite, zircon, and fergusonite structures. The linear variation of the cube root of the unit-cell volume with the tabulated radius of the A ion [Shannon (1976). *Acta Cryst.* A32, 751–767] has been evaluated. Within the rare-earth series, only the Gd compounds have cell volumes which deviate from straight-line behavior, a result which implies that r_{Gd} (CN = 8) should be 1·196 (1) Å. Systematic discrepancies are also noted for the corresponding Sc, Y, and La compounds which indicate that in these compounds the modified values of the radii should be r_{Sc} = 1·020 (2), r_Y = 1·154 (1), and r_{La} = 1·313 (2) Å. Literature cell constants have been used, in conjunction with the above analysis, to obtain radii for the analogous trivalent actinide ions, r_{Pu} = 1·250 (5), r_{Am} = 1·237 (5), and r_{Cm} = 1·224 (10) Å.

Introduction

The concept of an ionic, or crystal, radius is still a most useful one in understanding the structures and stabilities of complex oxide phases. Shannon & Prewitt (1969) and Shannon (1976) have been able to develop, in part by an analysis of experimentally determined lattice constants and unit-cell volumes, a systematic series of empirical radii for different valence and coordination states. Muller & Roy (1974) have related the occurrence of specific crystal structures in complex oxide phases $(A_xB_yO_z)$ to these radii by use of the structure-field map, where a stability

diagram is produced in which the coordinates of the phase space are the radii of the A and B ions.

As an initial phase of a program to focus in more detail on the concept of a structure-field map, precision lattice parameters have been determined for a series of $A^{3+}P^{5+}O_4$, $A^{3+}V^{5+}O_4$, and $A^{3+}Nb^{5+}O_4$ compounds where A is a rare-earth ion, scandium, yttrium, or lanthanum. Unit-cell volumes obtained from these lattice parameters have been analyzed in terms of the size of the A ion, and the results indicate that the radii of some of the A ions in these compounds may be different from the listed values (Shannon, 1976). Additional analysis of the unit-cell volumes of the analogous trivalent actinide compounds yields the corresponding radii of Pu, Am, and Cm in eightfold coordination.

The compounds used in this study were chosen, in part, because the structure-field map given by Muller & Roy (1974, Fig. 18) demonstrates a powerful systematization of the existing data, and because of the chemical and structural similarities between the phases that occur in this family of compounds. The monazite structure, which occurs primarily among the early lanthanide orthophosphates (prototype $CePO_4$), is monoclinic, space group $P2_1/n$. The zircon structure (prototype $ZrSiO_4$) is tetragonal, space group $I4_1/amd$, and occurs widely among the heavier lanthanide orthophosphates and arsenates, the lanthanide orthovanadates, and some actinide orthosilicates. The fergusonite structure (prototype $YNbO_4$) is monoclinic, space group $I2/c$, and occurs among the lanthanide (and actinide) orthoniobates and tantalates. Each of the three structure types contains isolated BO_4 tetrahedra interlinked by A ions which have primarily eightfold oxygen coordination. The structural and chemical similarities have been discussed elsewhere (Aldred, 1984).